

Figure S1 (Wu *et al.*)

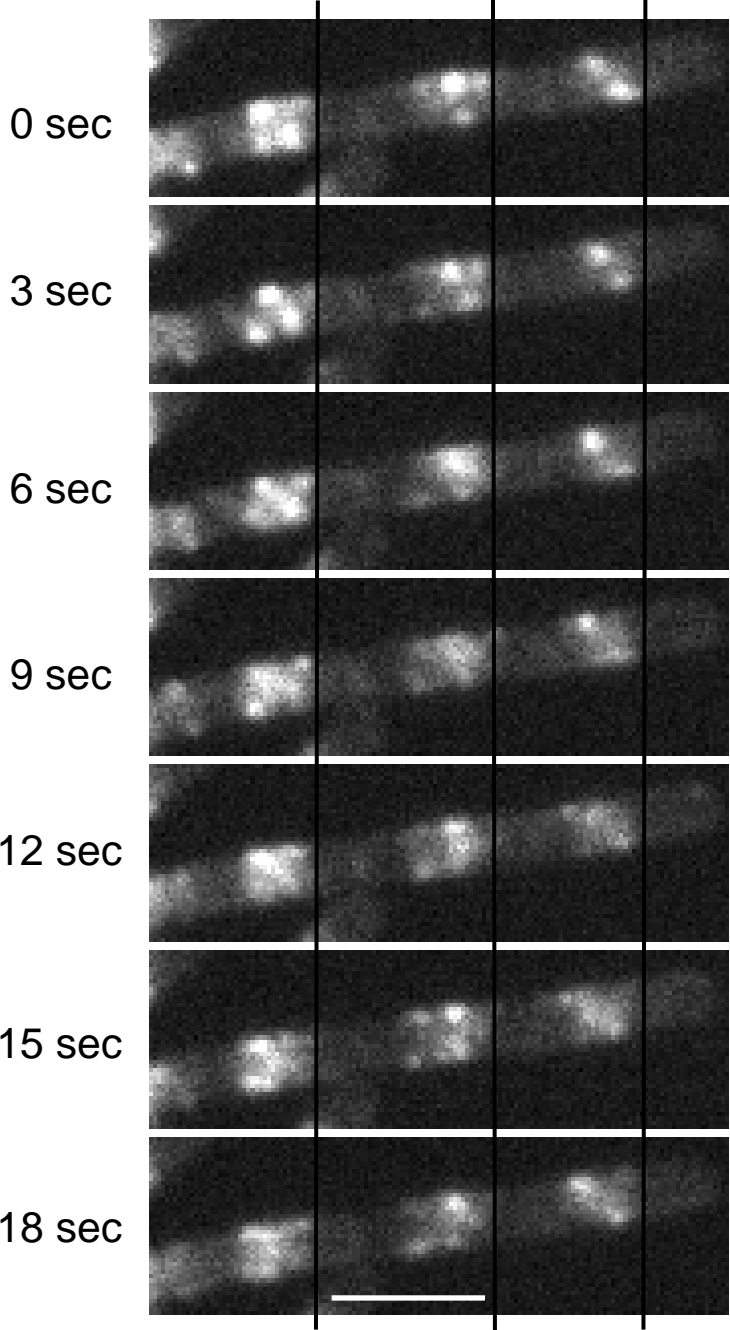
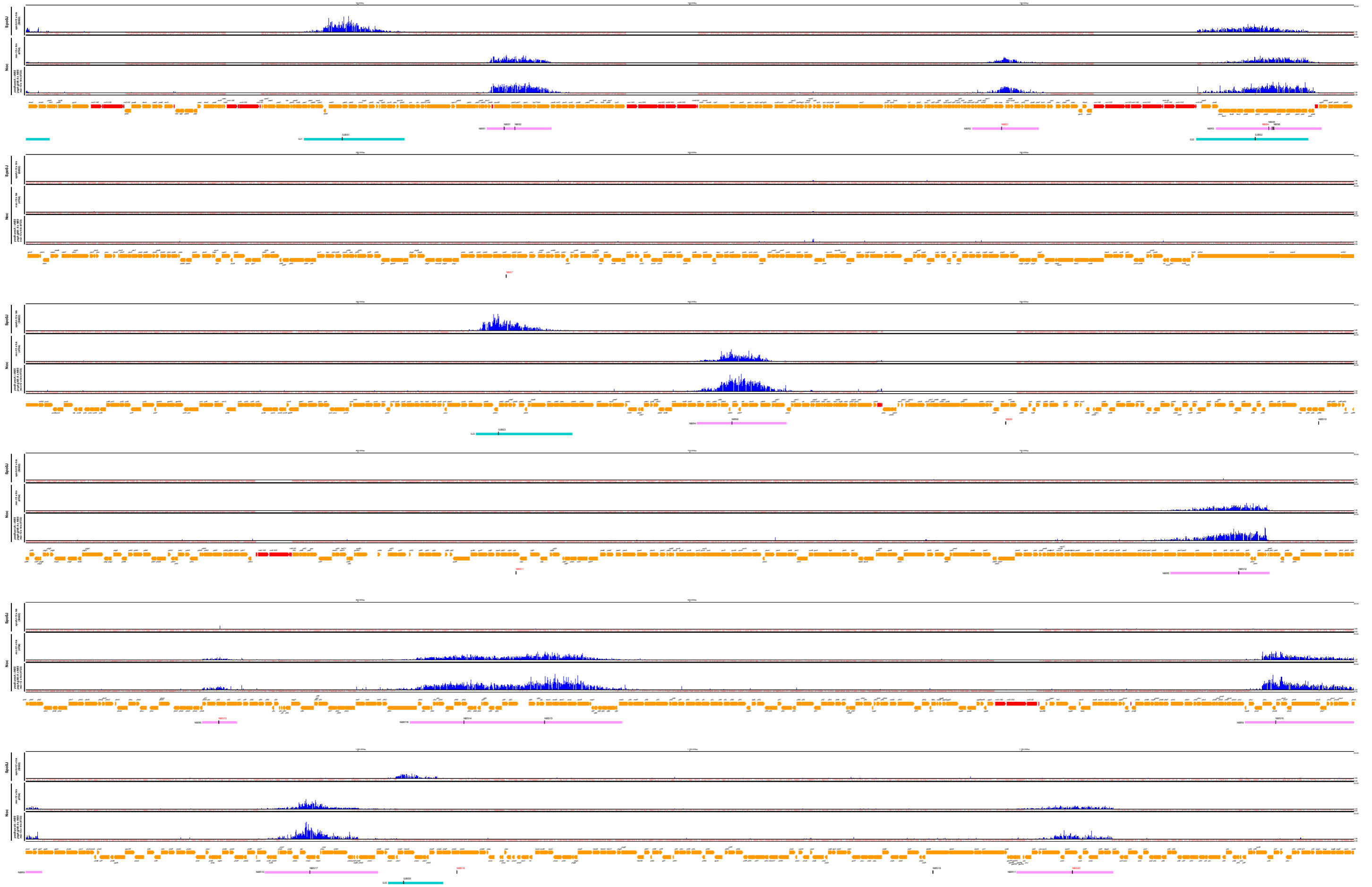
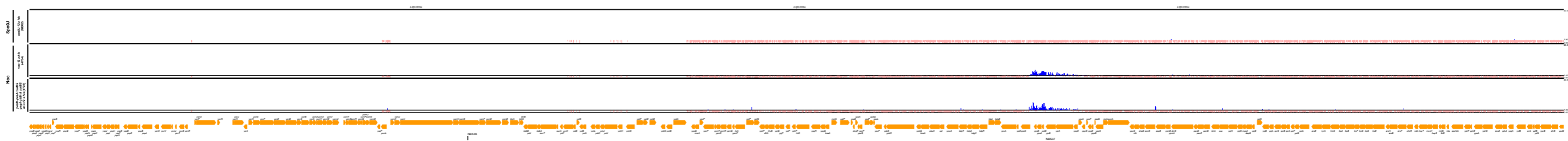
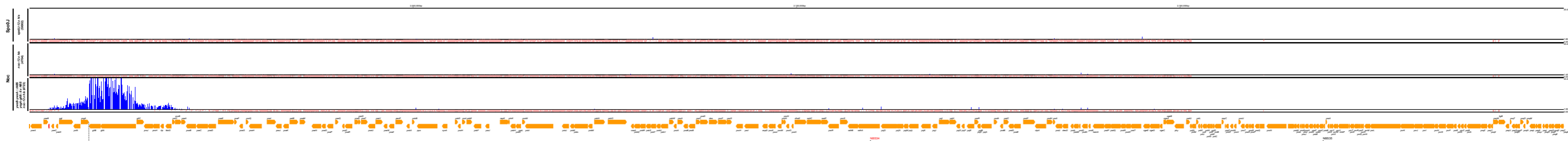
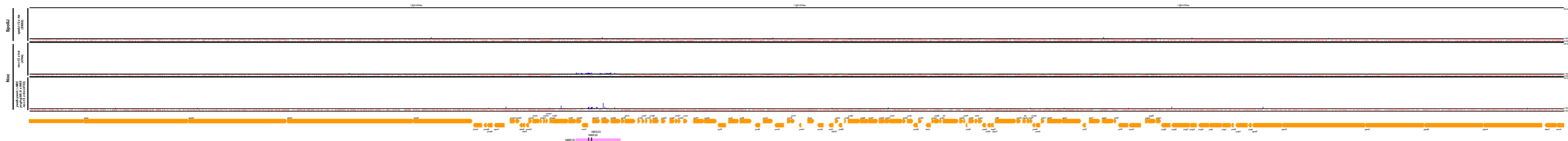
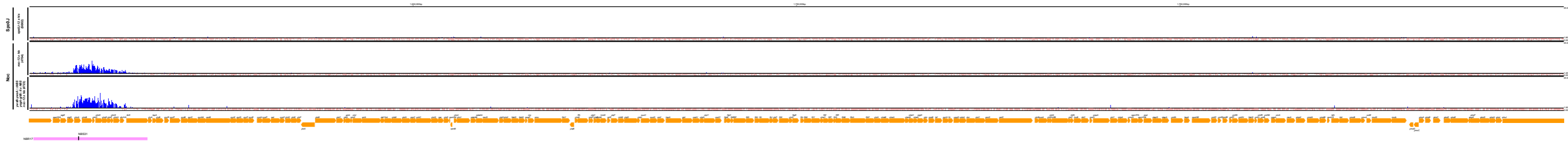
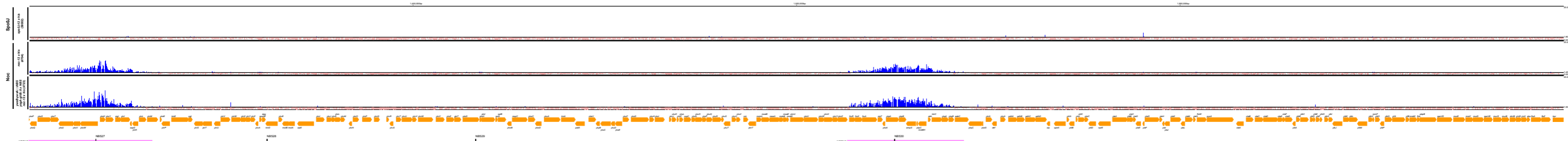
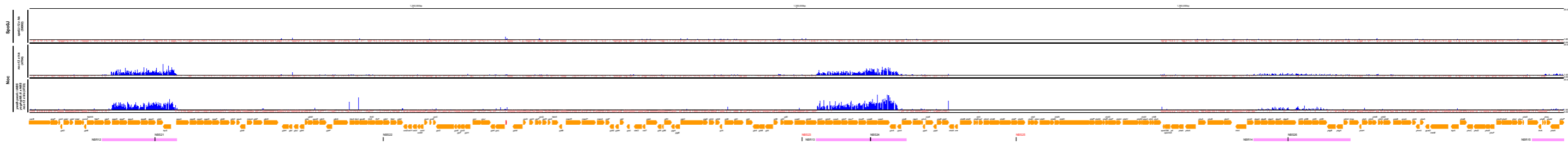
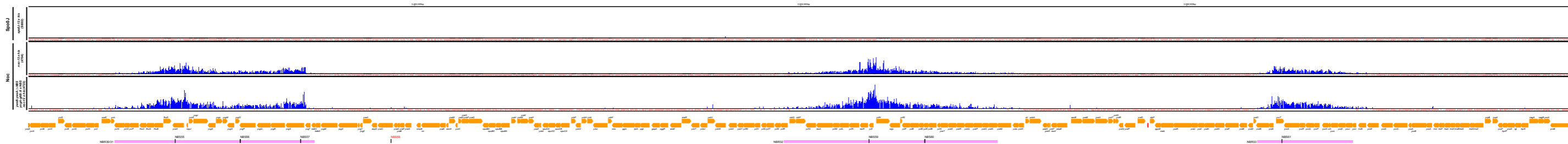
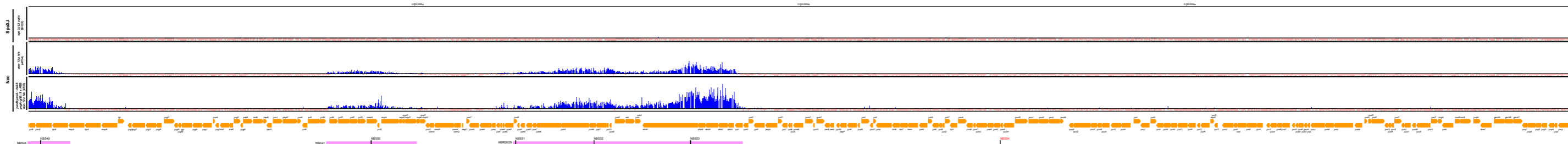
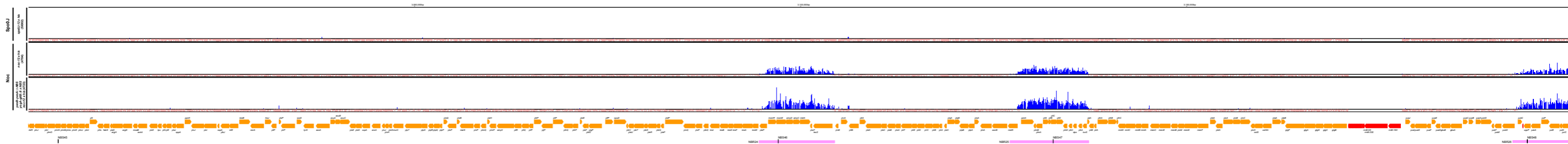
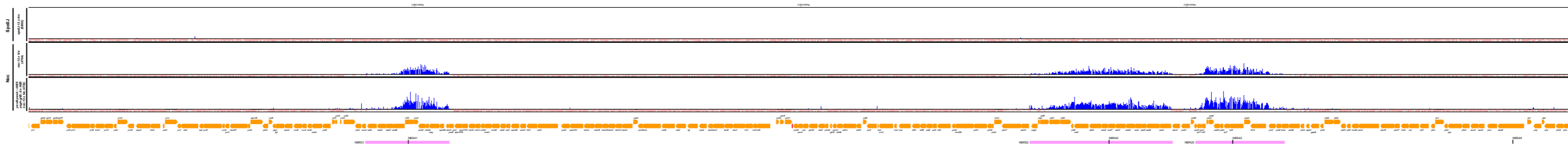
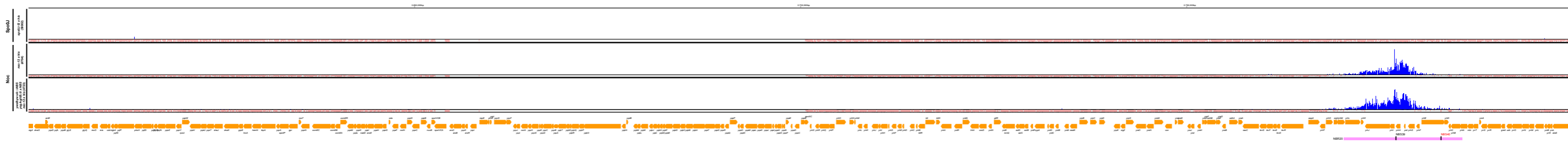
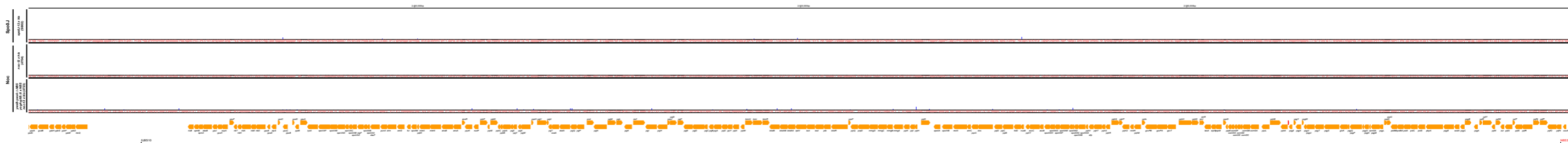
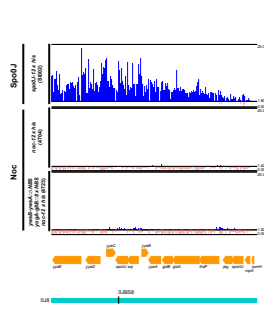
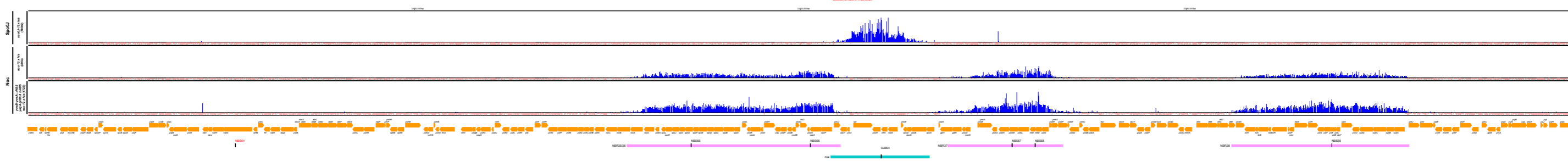
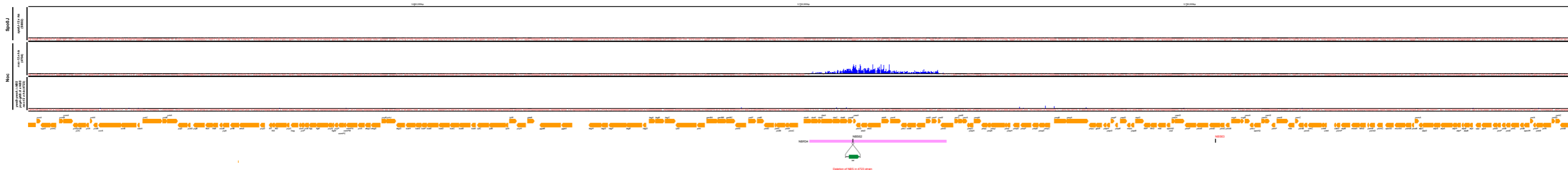


Fig S2 (Wu *et al.*)

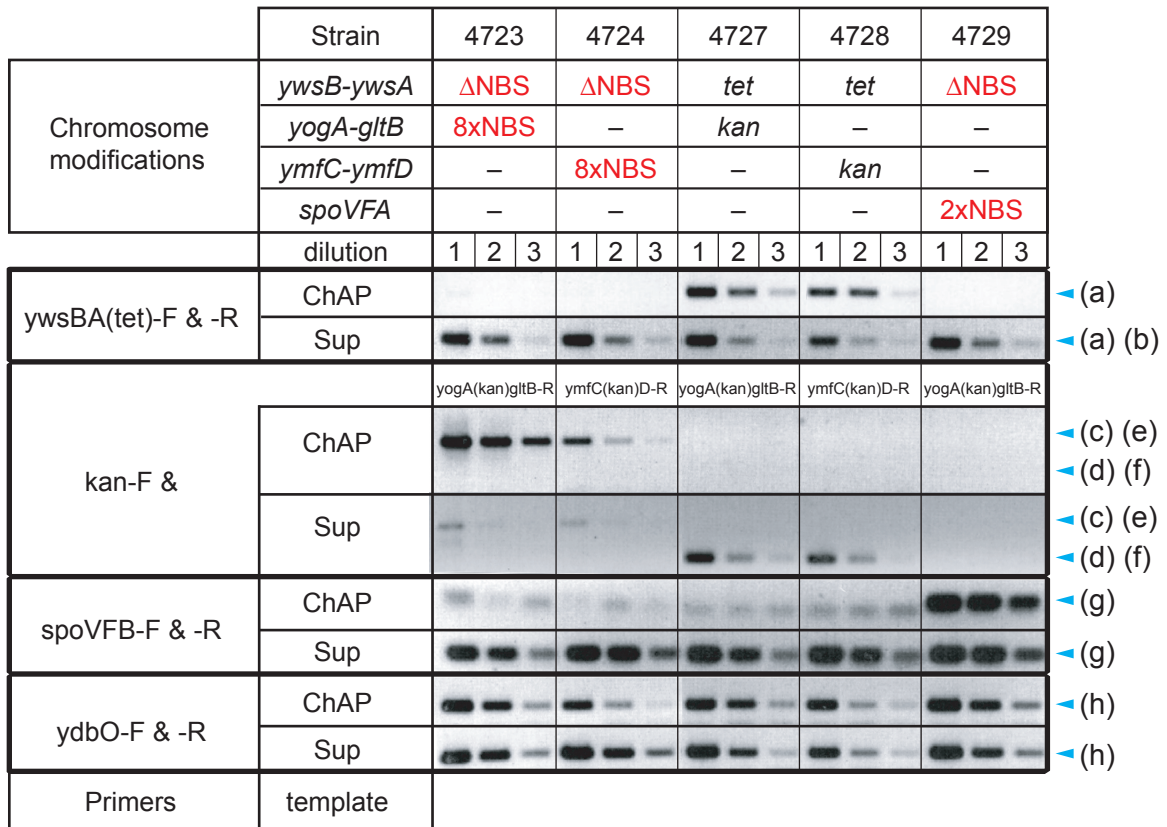








(A)



(B)

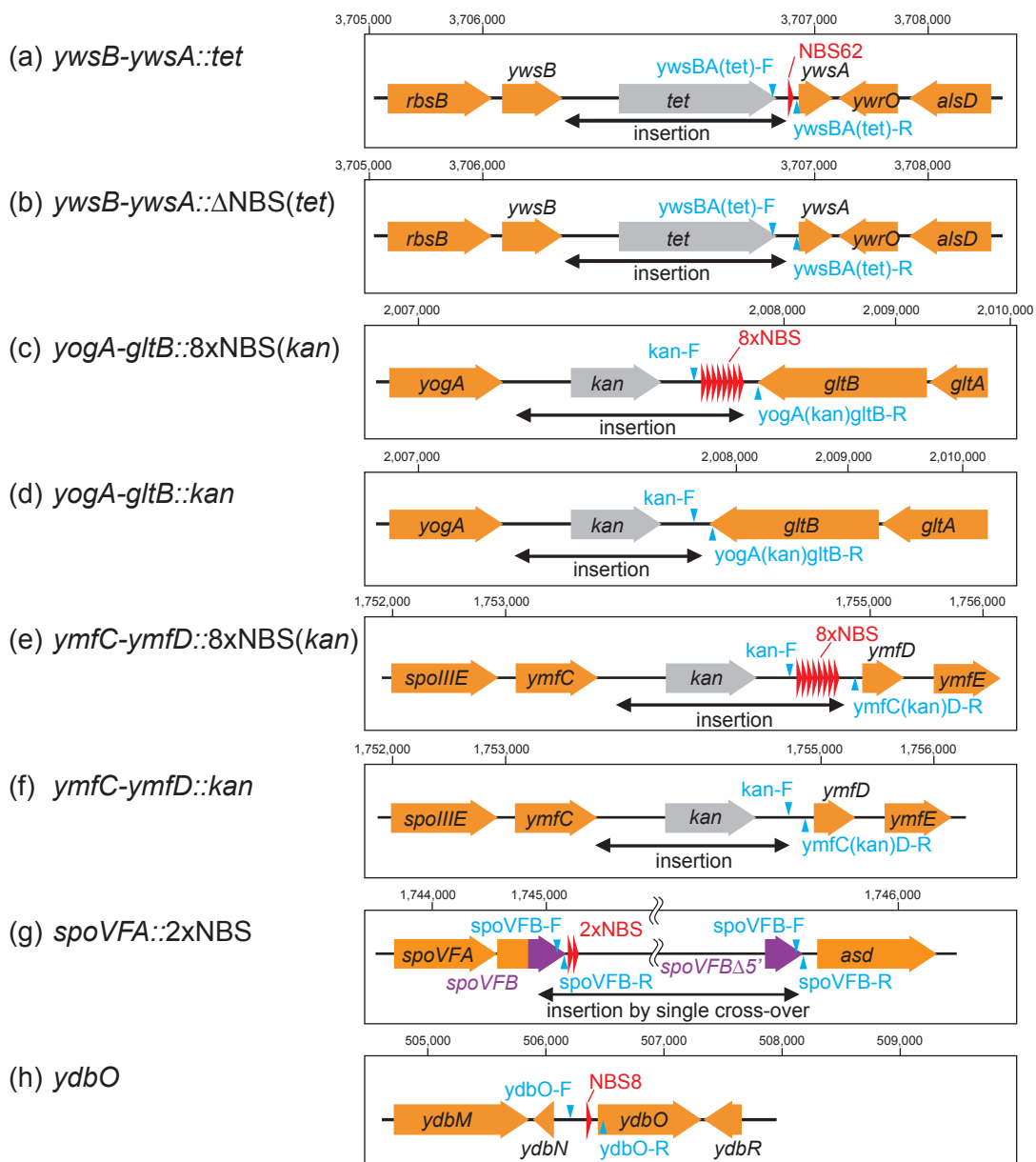


Fig S4 (Wu *et al.*)

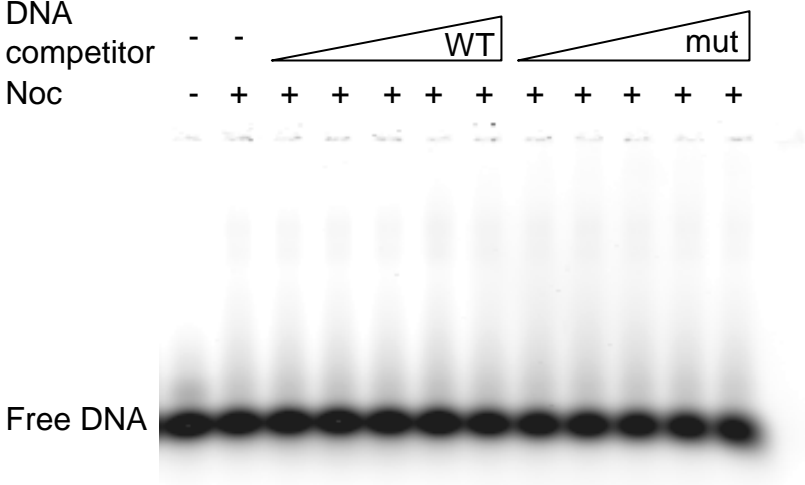


Figure S5 (Wu et al)

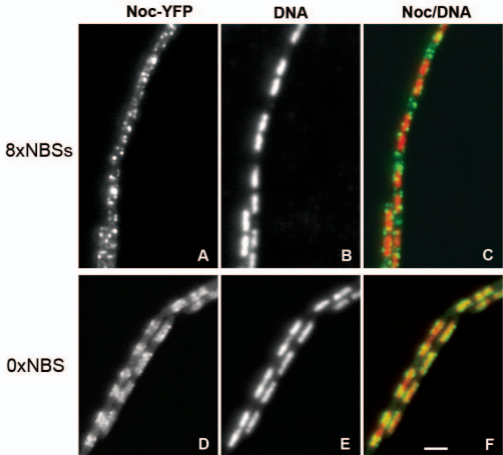


Table S1

	binding region ^a			binding sequence ^b						
	ID	start	end	length (kbp)	ID	PWM Score	sequence	other NBS ^c	start	end
Noc							ATTTC ^c CCCGGAAAT (consensus)			
	NBR1	69,424	79,118	9.7	NBS1	15.20	ATTTC ^c CCCGaGAAAa		72,015	72,028
					NBS2	16.44	ATTTC ^c CCCGGGAAAa	NBS43	73,631	73,644
	NBR2	142,528	152,527	10.0	<i>NBS3</i>	<i>14.87</i>	ATTgCgtGGGAAAT		146,960	146,973
					<i>NBS4</i>	<i>15.01</i>	ATTTtCaGGGAAAT		187,198	187,211
	NBR3	179,286	195,163	15.9	NBS5	15.56	ATgTCCCGGAAAT		187,701	187,714
					NBS6	16.18	ATTcCCtGGGAAAT	NBS24	187,956	187,969
	ND ^d				<i>NBS7</i>	<i>15.10</i>	ATTTCCttGGAAAg		272,185	272,198
	NBR4	501,045	514,543	13.5	NBS8	15.99	ATTgCCC ^c GGGAAAa		506,319	506,332
	(phage) ^e				<i>NBS9</i>	<i>15.10</i>	ATTTCCaaGGAAAa		547,503	547,516
	ND				NBS10	15.49	ATTgCCC ^c GAAAT		594,729	594,742
	ND				<i>NBS11</i>	<i>15.13</i>	ATTgCCaaGGgAAT		673,920	673,933
	NBR5	772,414	787,284	14.9	NBS12	16.47	ATTgCCC ^c GGGcAAT		782,691	782,704
	NBR6	826,549	831,774	5.2	<i>NBS13</i>	<i>14.92</i>	AaTcCCC ^c GGGAAAT		829,022	829,035
	NBR7	857,841	889,812	32.0	NBS14	15.97	ATTTc ^c CGGGAAAT	NBS 39, 68	865,963	865,976
	NBR8				NBS15	15.91	ATTTCCaaGGAAAT		878,110	878,123
	NBR9	983,632	1,002,353	18.7	NBS16	16.40	ATTTCCCGGGAAAa	NBS66	988,267	988,280
	NBR10	1,035,971	1,052,980	17.0	NBS17	15.54	ATTcCCgaGGAAAT		1,042,746	1,042,759
	ND				<i>NBS18</i>	<i>15.12</i>	tTTaCCC ^c GGGAAAa		1,064,797	1,064,810
	ND				NBS19	15.60	ATTgCt ^c CGGGAAAT		1,136,603	1,136,616
	NBR11	1,149,211	1,163,760	14.6	<i>NBS20</i>	<i>14.91</i>	ATTTCCCGGcAAAa		1,157,631	1,157,644
	NBR12	1,209,448	1,219,187	9.7	NBS21	15.16	ATagCCC ^c GGGAAAT		1,216,340	1,216,353
	ND				NBS22	15.69	ATTgCCC ^c GGGcAAAa		1,246,089	1,246,102
	ND				<i>NBS23</i>	<i>14.92</i>	ATTaCCC ^c GGgAAAa		1,300,864	1,300,877
	NBR13	1,302,538	1,314,295	11.8	NBS24	16.18	ATTcCCtGGGAAAT	NBS6	1,309,612	1,309,625
	(phage)				<i>NBS25</i>	<i>15.04</i>	ATTTCCacGGAAAa		1,327,478	1,327,491
	NBR14	1,359,589	1,372,178	12.6	NBS26	15.66	ATTTaCCGGGAAAT		1,364,056	1,364,069
	NBR15	1,395,873	1,416,015	20.1	NBS27	16.74	ATTaCCC ^c GGGAAAT		1,408,639	1,408,652
	ND				NBS28	15.35	ATTTCCtGaGAAAT	NBS36,62,73	1,430,963	1,430,976
	ND				NBS29	16.10	ATTaCCgGGGAAAT		1,458,161	1,458,174
	NBR16	1,506,620	1,521,783	15.2	NBS30	16.57	ATTTCCgGGGAAAT	NBS70	1,512,772	1,512,785
	NBR17	1,600,540	1,615,333	14.8	NBS31	16.07	ATTgCCC ^c GGGAAAa		1,606,379	1,606,392
	NBR18	1,871,232	1,877,034	5.8	NBS32	15.16	ATTTc ^c CGGGAAAa	NBS33	1,872,877	1,872,890
					NBS33	15.16	ATTTc ^c CGGGAAAa	NBS32	1,873,274	1,873,287
	ND				<i>NBS34</i>	<i>14.97</i>	ATTcCCtGGGgAAG		2,109,707	2,109,720
	(phage)				NBS35	16.03	ATTTCCCGGGcAAG		2,168,634	2,168,647
	(phage)				NBS36	15.35	ATTTCCtGaGAAAT	NBS28,62,73	2,257,123	2,257,136
	NBR19	2,330,277	2,337,738	7.5	NBS37	16.00	ATTcCCC ^c GGGAAAa		2,332,505	2,332,518
	ND				<i>NBS38</i>	<i>14.96</i>	ATTgCCGgAaGAAAT		2,598,414	2,598,427
	NBR20	2,770,362	2,785,662	15.3	NBS39	15.97	ATTTc ^c CGGGAAAT	NBS14, 68	2,777,087	2,777,100
	ND				<i>NBS40</i>	<i>14.92</i>	ATTTCCgGaGgAAT		2,782,892	2,782,905
	NBR21	2,843,648	2,854,479	10.8	NBS41	15.48	ATTaCCgaGGAAAT		2,849,169	2,849,182
	NBR22	2,929,677	2,948,154	18.5	NBS42	16.34	ATTaCCC ^c GGGgAAT		2,939,921	2,939,934
	NBR23	2,951,132	2,962,647	11.5	NBS43	16.44	ATTTCCCGGGAAAa	NBS2	2,955,940	2,955,953
	ND				NBS44	15.31	ATTgCCC ^c GaAAAT	NBS45	2,992,211	2,992,224
	ND				NBS45	15.31	ATTgCCC ^c GaAAAT	NBS44	3,003,833	3,003,846
	NBR24	3,094,616	3,104,422	9.8	NBS46	16.22	ATTgCctGGGAAAT		3,097,098	3,097,111
	NBR25	3,127,110	3,137,321	10.2	NBS47	16.53	ATTTCCaGGGAAAT		3,132,695	3,132,708
	NBR26	3,192,210	3,205,375	13.2	NBS48	15.83	ATTgCCgGGGcAAT		3,194,104	3,194,117
					NBS49	16.20	ATTgCCgGGGAAAT		3,201,557	3,201,570
	NBR27	3,238,587	3,250,257	11.7	NBS50	15.79	ATTgCCgGGGgAAT		3,244,378	3,244,391

NBR28	3,262,776	3,292,455	29.7	NBS51	15.68	ATTT g CCGGGAAAT	3,263,064	3,263,077	
				NBS52	15.81	ATTTCC CCa GGAAA a	3,273,229	3,273,242	
NBR29				NBS53	17.21	ATTTCCCGGGAAAT	3,285,728	3,285,741	
ND				<i>NBS54</i>	<i>15.10</i>	ATTTCC ga GGAAA c	3,325,833	3,325,846	
NBR30				NBS55	15.31	ATT gt CCGGGAAAT	3,418,984	3,418,997	
NBR31	3,411,168	3,437,030	25.9	NBS56	15.56	AT g TCCCGGGAAAT	3,427,425	3,427,438	
				NBS57	15.41	ATT c CC CCa GGAAA a	3,435,226	3,435,239	
ND				<i>NBS58</i>	<i>15.13</i>	ATTTCC tt GGAAA a	3,447,075	3,447,088	
NBR32	3,497,825	3,525,469	27.6	NBS59	16.84	ATT g CCCGGGAAAT	3,508,841	3,508,854	
				NBS60	15.82	ATTTCC t GGGAAA a	3,516,074	3,516,087	
NBR33	3,559,126	3,571,479	12.4	NBS61	16.03	ATTTCCCGGGGAA a	3,562,307	3,562,320	
NBR34	3,701,174	3,718,878	17.7	NBS62	15.35	ATTTCC tGa GAAATNBS28,36, 7:	3,706,775	3,706,788	
ND				<i>NBS63</i>	<i>15.02</i>	ATT c CC CCg CCAA a	3,753,679	3,753,692	
ND				<i>NBS64</i>	<i>14.94</i>	ATT c cttGGGAAAT	3,826,860	3,826,873	
NBR35				NBS65	15.28	ATT ct CCCGGGAAAT	3,885,840	3,885,853	
NBR36	3,877,522	3,905,167	27.6	NBS66	16.40	ATTTCCCGGGAAA g NBS16	3,901,296	3,901,309	
NBR37	3,919,086	3,933,964	14.9	NBS67	15.80	ATTTCC g GGGAAA a	3,927,398	3,927,411	
				NBS68	15.97	ATTT ct CGGGAAAT NBS14, 39	3,930,376	3,930,389	
NBR38	3,955,818	3,978,799	23.0	NBS69	15.35	ATTT ctt GGGAAAT	3,968,799	3,968,812	
NBR39	4,029,664	4,049,613	20.0	NBS70	16.57	ATTTCC g GGGAAAT NBS30	4,038,650	4,038,663	
				NBS71	15.31	ATT g CC ct GGAAA c	4,041,348	4,041,361	
NBR40	4,085,587	4,092,485	6.9	NBS72	15.29	ATTTCC aGa GAAAT	4,089,302	4,089,315	
NBR41	4,129,017	4,143,359	14.3	NBS73	15.35	ATTTCC tGa GAAATNBS28,36, 6:	4,136,398	4,136,411	
ND				NBS74	15.54	ATT g CC aa GGAAAT	4,150,991	4,151,004	
Spo0J ^f						TGTTTCACGTGAAACA (consensus)			
OJ1	41,890	57,001	15.1	OJBS1	23.21	TGTT a CACGTGAA ACA	47,640	47,655	
OJ2	176,308	193,136	16.8	OJBS2	23.10	TGTT a CACGTG tA ACA	185,161	185,176	
OJ3	467,785	482,280	14.5	OJBS3	21.88	c GT Tc CA t GTGAA ACA	471,151	471,166	
OJ9	1,054,553	1,062,814	8.3	OJBS9	21.13	a GT cc Ca T GAA AC g	1,056,855	1,056,870	
ND				OJBS10	20.20	TGTT c CA taa GAA ACA	2,414,565	2,414,580	
OJ4	3,903,912	3,916,703	12.8	OJBS4	23.21	TGTT a CACGTGAA ACA	OJ5	3,910,454	3,910,469
OJ5				OJBS5	23.21	TGTT a CACGTGAA ACA	OJ4	4,146,458	4,146,473
OJ6	4,128,420	4,174,412	46.0	OJBS6	22.71	c GT TTc ACGTGAA ACA	4,151,806	4,151,821	
OJ7				OJBS7	22.57	TGTT TCa t GTGAA ACA	4,165,780	4,165,795	
OJ8	4,187,425	3,529	30.7	OJBS8	23.24	TGTT c CACGTGAA ACA	4,204,760	4,204,775	

^a Peaks of Noc- and Spo0J-binding regions were automatically detected by the methods as described in materials and methods. Note that some peaks NBR7 & 8, NBR28 & 29, NBR30 & 31, NBR35 & 36 and OJ05, 06 & 07 were merged.

^b Bases different from the predicted consensus binding sequences are indicated in red; NBSs with PWM score values < 15.15 are

^c ID of NBS at other genome position is shown if exist.

^d Not detected.

^e The GeneChip used in this study does not have probes in phage-related regions.

^f Spo0J-binding peaks were detected by using data set previously published (Ishikawa et al., 2007).

Supplemental Data

Figure S1 Dynamic localization of Noc-YFP captured using timelapse microscopy.

Strain 4702 with a *noc-yfp* fusion (and without the native *noc*) growing exponentially in CH medium containing 0.3 % xylose was imaged at 28°C using a Spinning Disc Confocal System. The black lines mark the left or the right edge of the YFP signals at the beginning of the timelapse experiment (t0). Scale bar, 2 μm.

Figure S2 DNA binding profiles of Spo0J and Noc proteins on the *B. subtilis* genome revealed using ChAP-chip analysis. Binding signals of Spo0J (SI002, top), and Noc in a wild-type strain (4704, middle) and in a mutant strain with NBS-insertion at *yogA* region and deletion at *ywsA* region (4723, bottom) are shown. Top and bottom lines indicate signal intensities of 20 and 0 respectively. Middle lines exhibit threshold values to detect binding regions. Noc and Spo0J binding regions detected by our algorithm are shown as pink and green boxes with IDs, respectively. Positions of Noc binding sequence (NBS) with high score of PWM value and Spo0J binding sequence (*parS*) are also indicated by vertical lines under gene map. The insertion of 8 copies of NBS between *yogA* and *gltB*, and the deletion of NBS by replacing with a *tet* cassette between *ywsB* and *ywsA* in strain 4723 are also indicated.

Figure S3 Enrichment of DNA at selected NBRs as detected by ChAP using specific primer pairs. (A) ChAP analysis of the various strains harbouring an NBS deletion and /or insertion. Modified chromosomal regions are indicated in the upper part of the table. DNA fragments co-purified with Noc (ChAP) and total DNA extracted before ChAP-purification (Sup) were diluted 16-fold and 64-fold, respectively, and used as templates for quantitative PCR after a further 4-fold serial dilutions (lane 1, 2 and 3). Lower part of the panel shows the PCR products obtained with either the 'total' DNA (Sup), or ChAP-

purified DNA (ChAP), using primer pairs shown to the left. Two different reverse primers were used with kan-F and are indicated above the DNA bands. Primer pairs *ydbO-F* and *ydbO-R* are used to amplify the NBS located in the *ydbO* gene, which has been used for gel-shift assay (Figure 5). (B) Schematic map of the chromosomal regions that have been modified, showing the locations of the NBSs (in red), and the locations of the primers (in blue). a to h represent the PCR products obtained (in A) from the corresponding regions (in B).

Figure S4 Mutant protein Noc(K164A) is not able to bind the NBS in vitro. In the gel-shift assay the Noc(K164A)-12xHis was incubated with 25 nM of a Cy5-labelled probe containing the NBS from the *ydbO* gene. Unlabelled competitor DNA (wild type NBS or a mutant NBS) was present at concentrations of 0, 125 nM, 250nM, 500nM, 1 μ M or 2 μ M.

Figure S5 Localization of Noc-YFP in cells harbouring a multicopy plasmid carrying an NBS array (strain 4707; panels A-C) or without an NBS (strain 4706; panels D-F), grown in the presence of 0.3% xylose. A and D show the localization of Noc-YFP; B and E are images of nucleoids stained with DAPI; and C and F are overlaid images with Noc-YFP shown in green and DNA (DAPI) in red. Scale bar, 2 μ m.